agriculture

MDPI

Article

Quantifying and Mapping the Impact of Construction Land Expansion on Cultivated Land Fragmentation—A Case Study of Fuqing City, China

Xiaoran Yang [1], Xiping Zheng [1,2,*] and Xinyang Yu [1,3]

[1] College of Resources and Environment, Shandong Agricultural University, Tai'an 271018, China; yuxy.12b@igsnrr.ac.cn (Xinyang Yu)
[2] School of Surveying and Geoinformation Engineering, East China University of Technology, Nanchang 330013, China
[3] Institute of Geographic Sciences and Natural Resources Research, Chinese Academy of Sciences, Beijing 100101, China
* Correspondence: 2022120392@ecut.edu.cn

Abstract: To ensure the sustainable utilization of cultivated land resources, it is essential to quantify and map the characteristics of construction land and cultivated land and analyze the mechanisms by which construction land expansion affects cultivated land. However, few studies have been conducted focusing on this issue. This study integrated morphological spatial pattern analysis, spillover effect analysis, landscape pattern analysis, and a land use transition monitoring method to investigate the characteristics of construction land expansion and cultivated land fragmentation. Fuqing City of China was selected as the case study area for demonstration. The results demonstrated that the expansion of construction land resulted in fragmented patterns within the cultivated land landscape: (1) The large core area of cultivated land was subdivided into smaller core areas during 2000–2020, while the construction land exhibited a tendency towards aggregation and a spillover effect; (2) The expansion rate of the construction land in the study area accelerated, while the extent of the cultivated land decreased; (3) Cultivated land fragmentation intensified as landscape aggregation weakened, leading to an expansion in the agglomeration of construction land. The highlights of this study are: (1) examining the characteristics of construction land expansion and cultivated land fragmentation from morphological and geospatial perspectives; (2) categorizing the core areas of cultivated land based on their size to facilitate the analysis of factors contributing to cultivated land fragmentation. The findings in this study can be used to develop models to predict future patterns of cultivated and construction land to provide suggestions for landscape planning.

Keywords: cultivated land fragmentation; morphological spatial pattern analysis; landscape pattern index; land use transition; spillover effect

check for updates

Academic Editors: Johann G. Zaller and Xanthoula Eirini Pantazi

Received: 13 November 2024
Revised: 28 December 2024
Accepted: 13 January 2025
Published: 15 January 2025

Citation: Yang, X.; Zheng, X.; Yu, X. Quantifying and Mapping the Impact of Construction Land Expansion on Cultivated Land Fragmentation—A Case Study of Fuqing City, China. *Agriculture* **2025**, *15*, 184. https://doi.org/10.3390/agriculture15020184

Copyright: © 2025 by the authors. Licensee MDPI, Basel, Switzerland. This article is an open access article distributed under the terms and conditions of the Creative Commons Attribution (CC BY) license (https://creativecommons.org/licenses/by/4.0/).

1. Introduction

By the end of 2023, China's urbanization rate had reached 66.2%; industrialization and urbanization have facilitated the nation's rapid economic and social development. However, the expansion of construction land has led to a reduction in both the area and quality of cultivated land [1,2], thereby hindering agricultural modernization, weakening ecosystem services [3], and degrading the natural and economic quality of cultivated land [4]. In 1984, China established 14 coastal port cities [5]. Benefiting from a series of favorable policies, China's coastal regions have experienced significant industrialization and urbanization

during the past 20 years [6,7], resulting in the phenomenon of "non-agriculturalization" and severe "non-grainification" of cultivated land [8,9]. There is an urgent need to coordinate urban economic development with the protection of cultivated land.

Urbanization can result in significant landscape alterations [10,11]; cultivated land fragmentation is one of the main manifestations [12]. With an increasing awareness of the importance of preserving cultivated land, more and more scholars are conducting research on cultivated land conservation and food security from the perspective of changes in cultivated land landscapes. According to the landscape ecology hypothesis, the fragmentation of cultivated land can lead to an increase in both the quantity and density of cultivated land patches [13], and also result in a decrease in its connectivity and aggregation [14]. The fragmentation of cultivated land landscapes has been studied by scholars using landscape pattern index analysis [15,16], which provides an objective and quantitative representation of regional landscape fragmentation. However, the level of fragmentation in local areas is relatively weak and the spatial pattern of cultivated land landscape fragmentation cannot be accurately identified.

To accurately identify the spatial pattern of the local landscape, scholars have applied morphological spatial pattern analysis (MSPA) to identify ecological sources and landscape connectivity [17,18]. For instance, Ritters et al. analyzed the evolution of landscape patterns and extracted ecological sources in the study area based on MSPA [19]. Carlier and Moran used morphological spatial pattern analysis (MSPA) to study European greenways and found that greenways can provide green infrastructure and ecosystem connectivity, as well as enhanced landscape connectivity [20]. Ferrari et al. used the MSPA method to identify the key components of Rome's green infrastructure [21]. Shi et al. employed the MSPA approach and found that the amount of cultivated land in Kunming city was continuously declining, and that its spatial morphological change was stable, fluctuating, and then fragmenting [22]. Jiang studied the fragmentation of cultivated landscapes from urban to rural areas using the MSPA method and found that urban growth is the key cause of cultivated land fragmentation, and that land use policies have a significant impact on structural changes in cultivated land landscapes [23]. Javier Velázquez et al. used the MSPA method and the connectivity probability method to analyze the connectivity and fragmentation of forests and found that large core areas can significantly promote species exchange in the study area and nearby areas, and that bridging areas can enhance connectivity between patches, which is crucial for species conservation [17]. However, to the best of our knowledge, there is little research focusing on the impact of construction land expansion on cultivated land fragmentation based on a framework that combines MSPA and index methods. More in-depth research is urgently needed to determine the application range of a framework that integrates the advantages of MSPA in both spatial analysis and landscape pattern indices analysis.

This study thus selected a typical coastal city as the case study area and proposed a framework for geospatially identifying the impact of construction land expansion on cultivated land fragmentation during 2000–2020. The changing characteristics of the cultivated land spatial pattern were investigated with the aid of MSPA to carry out a thorough analysis of the cultivated land landscape change. The spillover effect analysis was used to measure the spatial correlation between construction land and cultivated land. The landscape pattern indices of the cultivated land and construction land were calculated to more accurately analyze the impact of construction land expansion on the landscape fragmentation of cultivated land, thereby distinguishing the effects of natural and economic factors in the study area. By using the aforementioned methods, the spatial and temporal characteristics and the influence mechanism of cultivated land fragmentation and construction land expansion were investigated to offer theoretical methodological

support and case references for ensuring food security and promoting harmonious social–economy–ecology development.

2. Materials and Methods

2.1. Study Area

The case study area is located on the southeast coast of China with a total area of 2430 km^2 (25°18′–25°52′ N, 119°03′–119°42′ E). It is the central region of the "21st-century sea silk road" and a well-known overseas Chinese township. With a GDP of 168.3 billion China Yuan, rising 4.9% annually, the study area ranked 14th out of the top 100 counties in China in 2023. The topography gently descends from the northwest to the southeast. The landscape consists primarily of low hills, with an average elevation of 500 m. To better study the construction land expansion and cultivated land fragmentation, the study area is divided into three parts: the central urban area, the north mountain area, and the south coastal area (Figure 1).

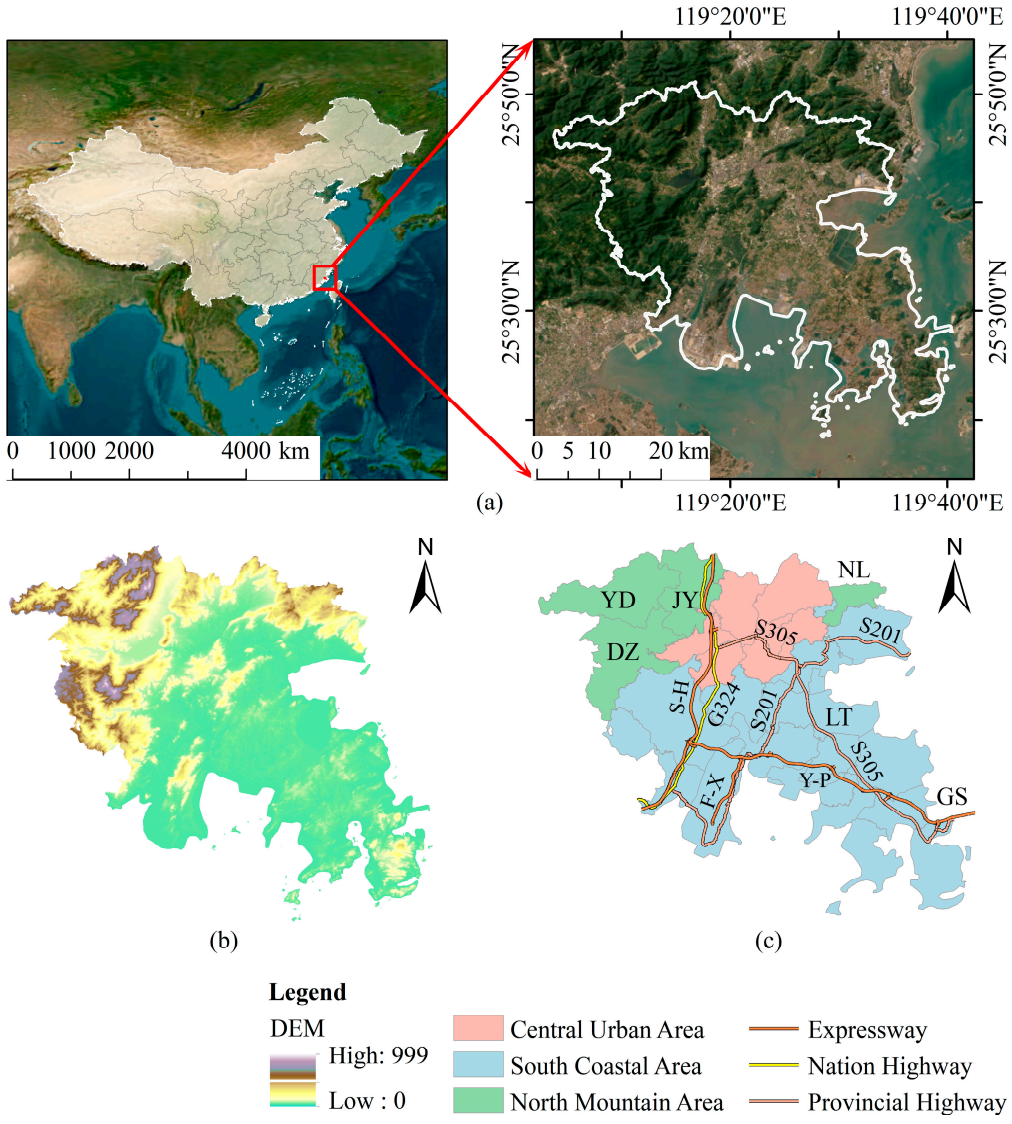


Figure 1. Location of the study area. (**a**): Location of the study area in China; (**b**): DEM of the study area; (**c**): Central urban area, north mountain area, and south coastal area in the study area, GS: Gaoshan Town, LT: Longtian Town, YD: Yidu Town, DZ: Dongzhang Town, NL: Nanling Town, JY: Jiangyin Town, S-H: Shenyang-Haikou Expressway, Y-P: Yuxi-Pingtan Expressway, F-X: Fuzhou-Xiamen Expressway.

2.2. Research Framework

This study proposed a framework for geospatially identifying the impact of construction land expansion on cultivated land fragmentation. The framework involved three major portions: dynamic change monitoring and MSPA methods were used to explore dynamic change monitoring of the cultivated land and the spatial pattern analysis of its morphology; spillover calculations and Moran's I calculation were employed to study the quantitative and spatial changes and spillover effect of the construction land; and land use transition and landscape pattern indexes were used to study the impact of construction expansion on cultivated land fragmentation (Figure 2).

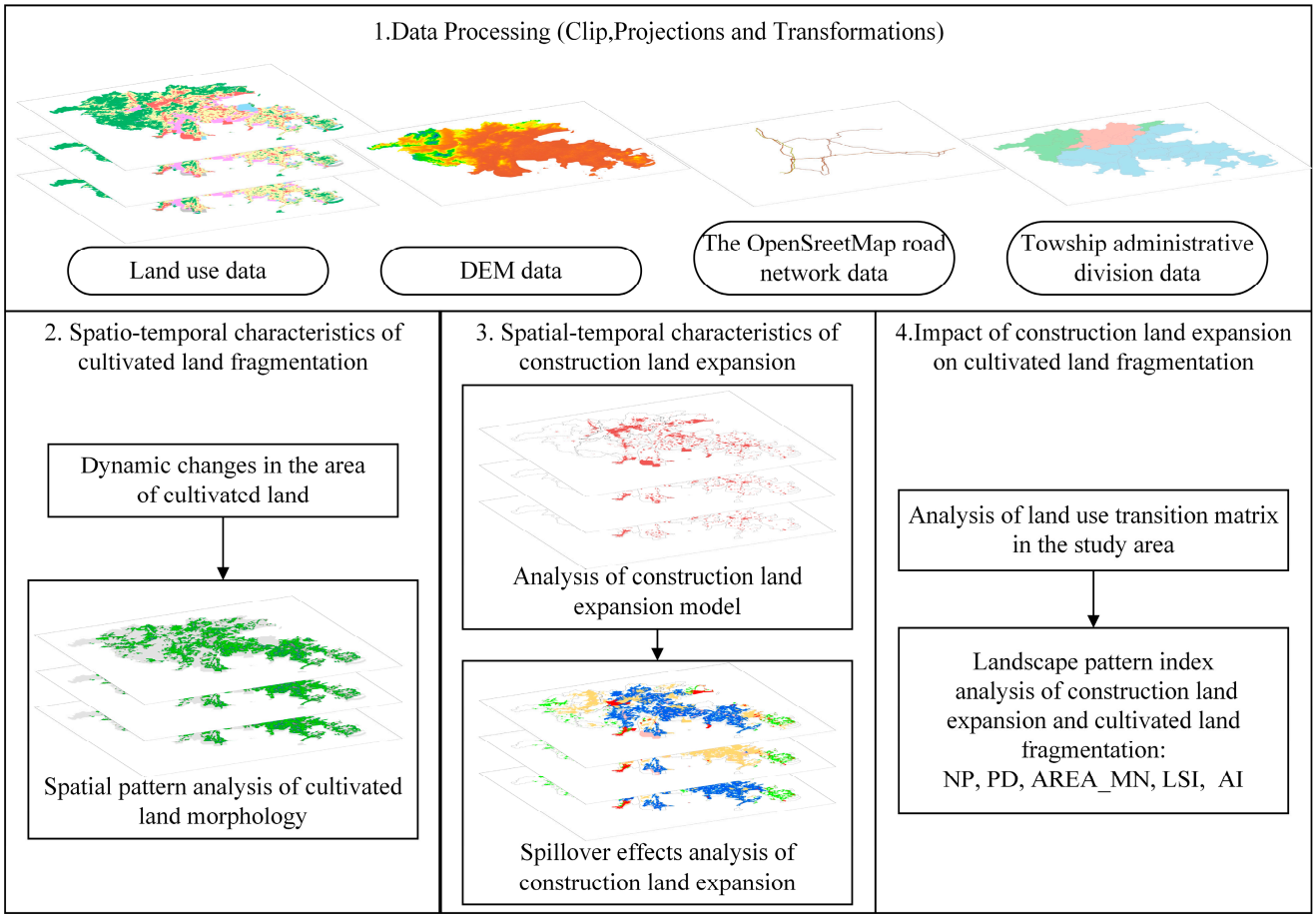


Figure 2. Study framework to explore the impact of construction land expansion on cultivated land fragmentation.

2.3. Data Processing

The land use data was acquired from GlobeLand30 (www.globeland30.org, accessed on 10 May 2022) with a spatial resolution of 30 m for the years 2000, 2010, and 2020. To ensure the accuracy of the subsequent analysis, these data were manually corrected and modified by referring to field survey data and Google high-resolution images. The improved classification data exhibited user's and producer's accuracies of 0.91–0.94 and 0.90–0.94 for the cultivated land and construction land, respectively. The township administrative boundary (vector data) and the DEM data (30 m) were obtained from the Geospatial Data Cloud (www.gscloud.cn, accessed on 10 May 2022). The road network data was from the OpenStreetMap (www.openstreetmap.org, accessed on 10 May 2022). Information about natural resources, geographic zoning, socioeconomics, and transportation was obtained from the local municipal government.

The data were processed using the following procedures (Figure 2):

(1) The spatial dataset was clipped, projected, and transformed using QGIS 3.30.0 software to ensure uniformity in the spatial reference coordinates of all the data, which were standardized as Xian_1980_3_Degree_GK_CM_120E. Based on the topographic conditions, the study area was divided according to township administrative divisions.

(2) Morphological spatial pattern analysis was conducted on the cultivated land by reclassifying land use data, assigning a value of 2 to cultivated land and 1 to other categories. The resulting dataset was then input into Guidos Toolbox 3.0 software to generate MSPA images specifically for cultivated land.

(3) The quantitative characteristics of the construction land and cultivated land were analyzed by processing three periods of land use data using QGIS software to calculate the area. The land use transition matrix from 2000 to 2010 and 2010 to 2020 was obtained, along with the dynamic change rates of the area for both construction and cultivated lands.

(4) The spillover effect of construction land expansion was analyzed by extracting the vector data of both the construction and cultivated land, utilizing Global Moran's I and Local Moran's I indices, selecting an inverse distance spatial relationship for analysis, and obtaining the spatial correlation types between the construction land and cultivated land.

(5) Landscape pattern indices analysis. Through geospatial analysis, the land use data were reclassified into cultivated land, woodland, grassland, waters (including wetlands, waterbody, and sea areas), construction land, and bare ground. Then, the land use reclassification results of three periods in each subdivision were input into Fragstats 4.2 software and the landscape pattern indices were calculated.

2.4. Methodology

(1) Morphological spatial pattern analysis (MSPA)

The MSPA method is a mathematical morphological approach for measuring, identifying, and segmenting binary images [24]. By processing the binarized land use image, it can help extract the core patch and establish a clear spatial topological relationship between the core element and other elements [25], resulting in seven distinct elements: the core, island, perforation, edge, loop, bridge, and branch [26,27]. This is the quantified description of the realization of landscape fragmentation (Table 1 and Figure 3).

Table 1. Landscape types and ecological implications of MSPA.

Landscape Type	Ecological Implications
Core	An internal precinct of the cultivated land landscape area.
Islet	The area is too small to form a cultivated land area in the core area, and it exists in isolation.
Perforation	The edge of the patch inside the core area, i.e., the transition area between the core area and the non-cultivated land area.
Edge	The junction line between the core area and the non-cultivated land area.
Loop	A narrow area that connects the same core area.
Bridge	A narrow area that connects at least two different core areas.
Branch	Only one end is connected to the edge zone, connecting bridge, loop, or core area.

(2) Landscape pattern analysis

The Landscape Pattern Index is utilized to quantitatively depict the characteristics and alterations in a landscape. This is primarily accomplished through Fragstats 4.2, which encompasses three distinct research scales: the patch index, type index, and landscape index. In this study, an analysis was conducted on each land use type's scale. Based on

the characteristics of the study area and in combination with previous research [28,29], the following indices were selected: NP, PD, AREA_MN, AI, and LSI (Table 2).

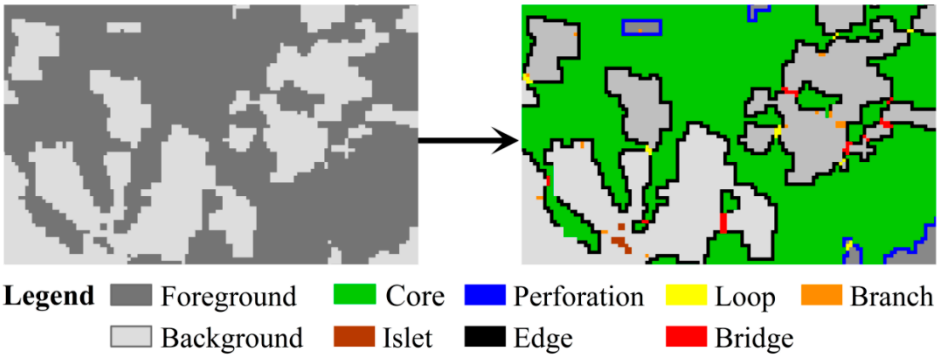


Figure 3. The landscape metrics map of MSPA.

Table 2. Description of the landscape index.

Index	Definition	Unit and the Range of Values
Number of patches (NP)	Type or number of patches in a landscape mosaic. The higher the value is, the more patches of this type it has.	pcs [1, +∞)
Patch density (PD)	The number of patches in the unit area (100 ha). The higher the value, the finer the patch segmentation.	Pcs/100 ha (0, +∞)
Patch Area_Mean (AREA_MN)	The area of each type of patch is averaged to describe the granularity of the landscape. The smaller the value is, the greater the degree of fragmentation is.	ha (0, +∞)
Aggregation index (AI)	Description of the extent to which landscape patches converge. The higher the value is, the better the aggregation is.	% (0, 100]
Landscape shape index (LSI)	Description of the characteristics of the shape of the patches within the entire landscape. The higher the value is, the more the patches are separated.	No units [0, +∞)

(3) Dynamic change rate of land use

The dynamic rate of changes in land use can be utilized as a tool for analyzing alterations within a specific land category over a given time frame. A higher value indicates a more intense transformation of the land type. The formula is:

$$V = \frac{L_b - L_a}{L_a \times T} \times 100\% \quad (1)$$

where L_a and L_b are the areas of a certain type of land in the a and b periods; T is the time interval between a and b periods, and the unit is years.

(4) Spillover effect analysis

Moran's I is utilized to analyze the spillover effect of construction land expansion. The Global Moran's I can indicate the spatial correlation between construction land and cultivated land in the study area, while the Local Moran's I can identify such correlations at a local scale [30,31]. Equation (2) represents the Global Moran's I, while Equation (3) denotes the Local Moran's I.

$$I = \frac{\sum_i \sum_j w_{ij} Z_i \cdot Z_j / S_0}{\sum_i z_i^2 / n} \quad (2)$$

$$I_i = \frac{Z_i}{S^2} \sum_{j \neq 0}^{n} w_{ij} Z_j (Z_i = y_i - \bar{y} Z_j = y_j - \bar{y} S^2 = \frac{1}{n} \sum (y_i - \bar{y})^2 S_0 = \sum_{i=1}^{n} \sum_{j=1}^{n} w_{ij}) \quad (3)$$

where n is the total number of patches; y_i and y_j indicate the land type of the ith and jth patches, respectively; w_{ij} is the spatial weight value. $I > 0$ represents a positive correlation,

$I < 0$ represents a negative correlation. The larger the absolute value of I is, the stronger the correlation is. $I_i > 0$ indicates the presence of spatially correlated aggregations, that is, the attribute values of the ith patch and its surroundings are high (high-high) or the attribute values for and around the ith patch are low (low-low). $I_i < 0$ means that there is no spatial homogeneity, that is, the attribute value of the ith patch is high but that of the surrounding patch is low (high-low), or the attribute value of the ith patch is low but that of the surrounding patch is high (low-high).

(5) Land use transition matrix

The land use transition matrix portrays the spatio-temporal fluctuations of diverse land use types, facilitating not only a quantitative description of land use characteristics within a fixed region over a specific period but also dynamic visualization of the direction, magnitude, and trend of transitions between different land use types.

3. Results

3.1. Spatio-Temporal Characteristics of Cultivated Land Fragmentation

3.1.1. Analysis of Dynamic Changes in Cultivated Land

During the study period, there was a noticeable decrease in cultivated land, with a significant acceleration during the second decade (Table 3). The largest reduction of cultivated land occurred along the south coastal area in the first decade. In contrast, during the second decade, the central urban area experienced the greatest loss of cultivated land, while a relatively low intensity of cultivated land loss was observed in the north mountain area throughout the entire study period.

Table 3. Change of cultivated land from 2000 to 2020.

Region	Period	Area Reduction (km^2)	Dynamic Change Rate (%)
Central urban area	2000–2010	2.83	0.24
	2010–2020	17.69	1.55
North mountain area	2000–2010	0.28	0.03
	2010–2020	3.37	0.36
South coastal area	2000–2010	19.16	0.41
	2010–2020	41.35	0.93
Total	2000–2010	22.27	0.33
	2010–2020	62.41	0.96

3.1.2. Spatial Pattern Analysis of Cultivated Land Morphology

Table 4 and Figure 4 presented the calculated area and dynamic change rate of each MSPA metric. The core zones exhibited the largest area among the foreground elements but showed a declining trend. Moreover, the rate of decline during the second decade surpassed that of the first. Conversely, islands, edges, bridges, and branches experienced an upward trend with a decelerated dynamic change rate in the second period. In contrast, perforations and loops gradually decreased at an accelerated pace during this time.

During the study period, the large core zones gradually fragmented into smaller ones, resulting in an increase in their amount. The connectivity between these core zones decreased while that of larger core zones with surrounding smaller ones strengthened. The cultivated land shape became more complex and its landscape increasingly fragmented.

Figure 5 illustrated seven types of raster images depicting conflicting landscape elements, generated by MSPA with cultivated land in the foreground. The color green represented the core, while varying shades from light to dark indicated a super-large core, large core, medium core, and small core, respectively. It can be found that the super-large core zone was distributed in the south coastal area, the large core zones were mainly

distributed in the north of the central urban area and the valley of the north mountain area, the medium core zones were mainly distributed in the peninsula of the south coastal area, and the small core zones were almost evenly distributed in all low-altitude areas. Hence, cultivated land fragmentation was more pronounced in mountain areas.

Table 4. The area and proportion of landscape elements in the study area.

Landscape Features	2000		2010		2020	
	Area (km^2)	Percentage (%)	Area (km^2)	Percentage (%)	Area (km^2)	Percentage (%)
Core	547.40	81.15	523.43	80.20	461.72	78.28
Islet	0.45	0.07	0.53	0.08	0.62	0.11
Perforation	33.49	4.97	27.30	4.18	21.66	3.67
Edge	80.44	11.92	87.09	13.34	91.59	15.53
Loop	2.21	0.33	2.08	0.32	1.75	0.30
Bridge	3.67	0.54	4.00	0.61	4.23	0.72
Branch	6.88	1.02	8.20	1.26	8.22	1.39
Total	674.54	100.00	652.62	100.00	589.80	100.00

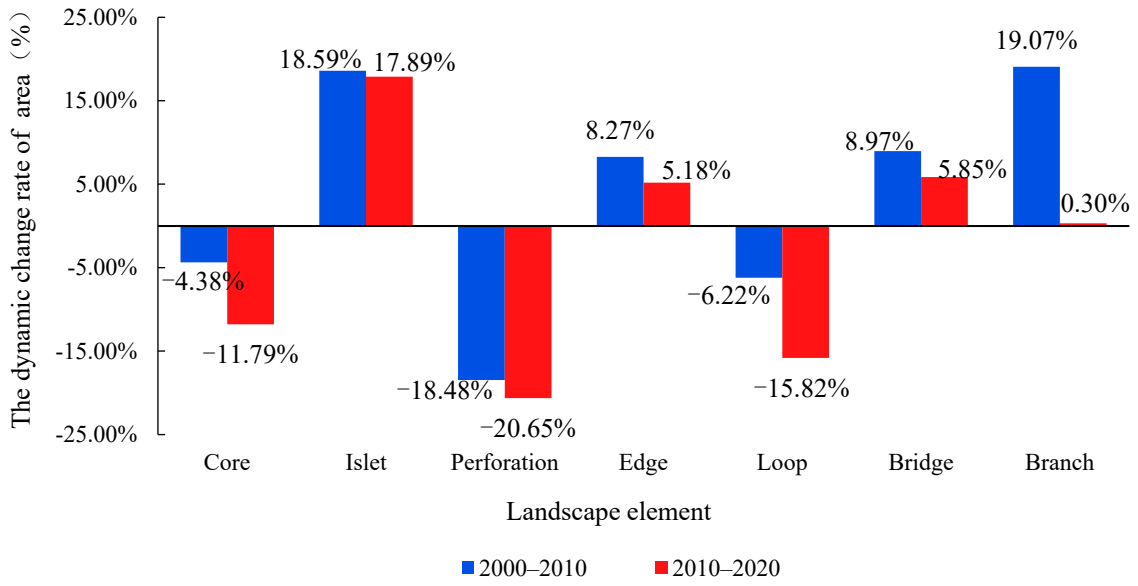


Figure 4. The dynamic change rate of landscape element area.

Considering the notable variations in both the number and size of cores across different regions, a reclassification of cores based on their areas was conducted: super-large core (≥100 km^2), large core (20~100 km^2), medium core (1~20 km^2), and small core (<1 km^2). Table 5 showed that the super-large core zone experienced a decrease followed by an increase during the study period, whereas the large core zones exhibited an initial increase and then a subsequent decrease, with a remarkably greater rate of decline than growth. The total area and the number of middle and small core zones exhibited an upward trend, with a higher growth rate observed in the second decade compared to the first. The larger core zones underwent gradual fragmentation into smaller ones, resulting in increased land use fragmentation within the study area.

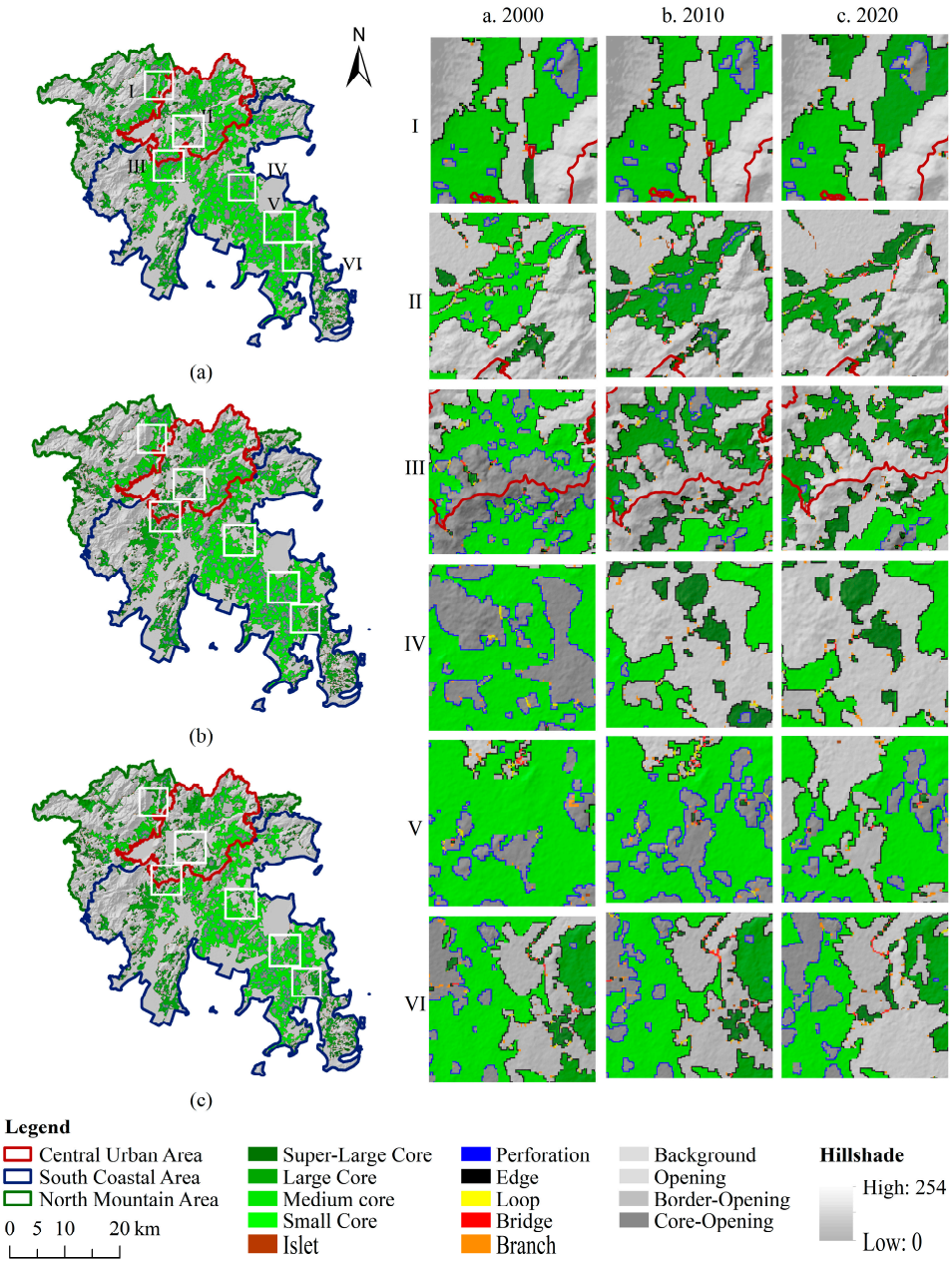


Figure 5. The morphological spatial pattern analysis of cultivated land in the study area: (**a**): 2000; (**b**): 2010; (**c**): 2020.

Table 5. The quantity, area, and proportion of each core area.

Core Area Classification	2000 Quantity (pcs)	2000 Area (km^2)	2000 Proportion (%)	2010 Quantity (pcs)	2010 Area (km^2)	2010 Proportion (%)	2020 Quantity (pcs)	2020 Area (km^2)	2020 Proportion (%)
Super-large core	1	328.48	60.01	1	215.37	41.15	1	234.47	50.78
Large core	2	80.67	14.74	3	136.68	26.11	2	41.76	9.04
Medium core	23	94.84	17.33	25	118.34	22.61	33	129.65	28.08
Small core	998	43.41	7.93	1056	53.04	10.13	1110	55.84	12.09
Total	1024	547.40	100.00	1085	523.43	100.00	1146	461.72	100.00

Table 5 showed that the area of the super-large core zone decreased significantly in 2010. Combined with Figure 5, it can be found that the super-large core zone is mainly divided into three parts (south, northeast, and northwest). The primary factor contributing to the fragmentation of the super-large core area in the northeast region is attributed to two changes as indicated in Figure 6. To more vividly explain the evolution process of

super-large cores, two representative sites (Site A and Site B) located in the northeast and northwest were selected in this study. In 2000, Site A was classified as a large cultivated land within the core zone according to MSPA analysis results. However, in 2010 and 2020, its size had diminished conspicuously, resembling more of a narrow bridge that separated Site A's left and right core zones into different areas. In 2000, Site B was characterized by cultivated land use, with construction lands on both sides. Consequently, the cultivated land at Site B formed a narrow strip that connected the upper and lower core zones, appearing as an island in the MSPA analysis results. By 2010, however, the expansion of construction lands around Site B had led to a decrease in the cultivated land area such that it now forms a bridge according to MSPA analysis. In 2020, a portion of the construction land at site B was converted into cultivated land, increasing the area of cultivated land. The MSPA analysis revealed that this area served as a core zone, connecting both the upper and lower core zones and merging them into one cohesive unit. According to the road network data, the primary factor contributing to the fragmentation of the super-large core zone in the northwest was attributed to the construction of the G324 national highway. Furthermore, there was a noticeable expansion trend observed in construction land near the G324 national highway, which further diminished and severed its super-large core.

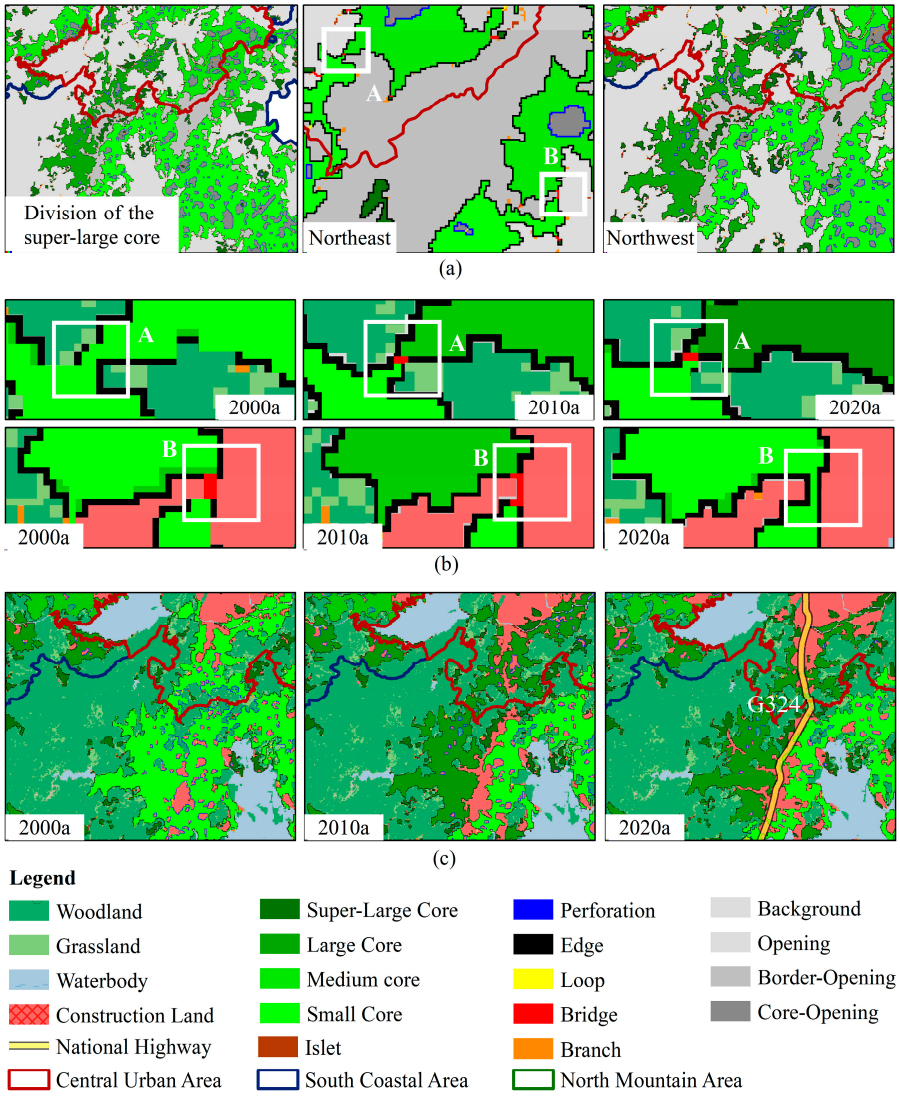


Figure 6. The evolution process of the super-large core areas: (**a**): 2010 super-large core partitions; (**b**) Evolution of the super-large core area in the northeast; (**c**): The evolution of the super-large core area in the northwest.

3.2. Characteristics of Construction Land Expansion

3.2.1. Analysis of Construction Land Expansion

Construction land in the study area continued to expand during the study period with a trend of accelerating expansion. Especially in the north mountain area, there was slow and weak expansion during the first decade. However, from 2010 to 2020, there was a significant increase in the dynamic change rate of construction land expansion, indicating a rapid expansion trend (Table 6). The dynamic change rate of construction land expansion in the south coastal area consistently exceeded that of the overall level.

Table 6. Change of construction land from 2000 to 2020.

Region	Period	Expansion Area (km^2)	Change Rate (%).
Central urban area	2000–2010	3.80	1.07
	2010–2020	16.65	4.22
North mountain area	2000–2010	0.35	0.55
	2010–2020	3.32	5.04
South coastal area	2000–2010	22.51	2.70
	2010–2020	52.81	4.98
Entire study area	2000–2010	26.66	2.13
	2010–2020	72.78	4.79

Figure 7 showed the spatial distribution of construction land in the study area. The urban construction land radiated outward from the city center, with a slow expansion in the first decade followed by rapid growth in the second. The opening of the Fuqing Railway Station in 2010 spurred swift economic development and the consequent expansion of construction land in the eastern suburbs. Meanwhile, to the southwest of the central urban area, the construction land has expanded along a strip adjacent to the G104 national highway. The expansion of construction land in the north mountain area was relatively limited during the first decade. However, there was a concentrated distribution of construction land near the G324 national highway through Jingyang Town, which serves as an industrial concentration zone for this town. Following the opening of the Shenhai Expressway in 2017, industrial enterprises within Jingyang Town experienced rapid development and a subsequent expansion of construction land. Similarly, Yidu Town (YD in Figure 7) and Dongzhang Town (DZ) also witnessed significant growth in their respective construction lands. In the south coastal region, there has been a significant expansion of construction land over the past two decades, taking on three primary forms: linear slow expansion along routes, such as the S201 and S305; marginal types of slow expansion in areas, like Longtian Town (LT), Gaoshan Town (GS), and scattered rural settlements; and flaky concentration expansion in zones like the Yuanhong Investment Zone (YH) and Jiangyin Economic Zone (JY). In conclusion, the primary factors contributing to the expansion of construction land were road construction and urban development planning. Additionally, topography served as a significant constraint on such expansion.

3.2.2. Spillover Effects of Construction Land Expansion

Based on the Global Moran's *I* analysis of construction land and cultivated land during the study period, the average value of Moran's I is 0.22 with a confidence level of 99%. The results indicate that there is a spillover effect from construction land to cultivated land in the study area (see Figure 8). The following analysis provides further details:

The results of the Local Moran's I analysis indicated that in 2000, there was a significant concentration of construction land in the downtown area, which subsequently led to an expansion of construction land in nearby regions. This spillover effect exhibited a "High-High Cluster" pattern. However, due to their distance and hilly terrain, the suburbs experienced weakened spillover effects and mostly displayed "Low-High Outlier" patterns. In 2010, the spillover effect of construction land was particularly pronounced

in the eastern valley of the central urban area, characterized by a "High-High Cluster", while no significant spatial correlation between construction land and cultivated land was observed in other regions. By 2020, however, this correlation had strengthened outside the city center. In the valley with a higher concentration of construction land, the spillover effect exhibited a "High-High Cluster", while in the surrounding areas, it weakened to a "Low-High Outlier", due to distance and topography. The northwest region of the central urban area is adjacent to mountains and water bodies, resulting in weaker spillover effects due to topographical factors.

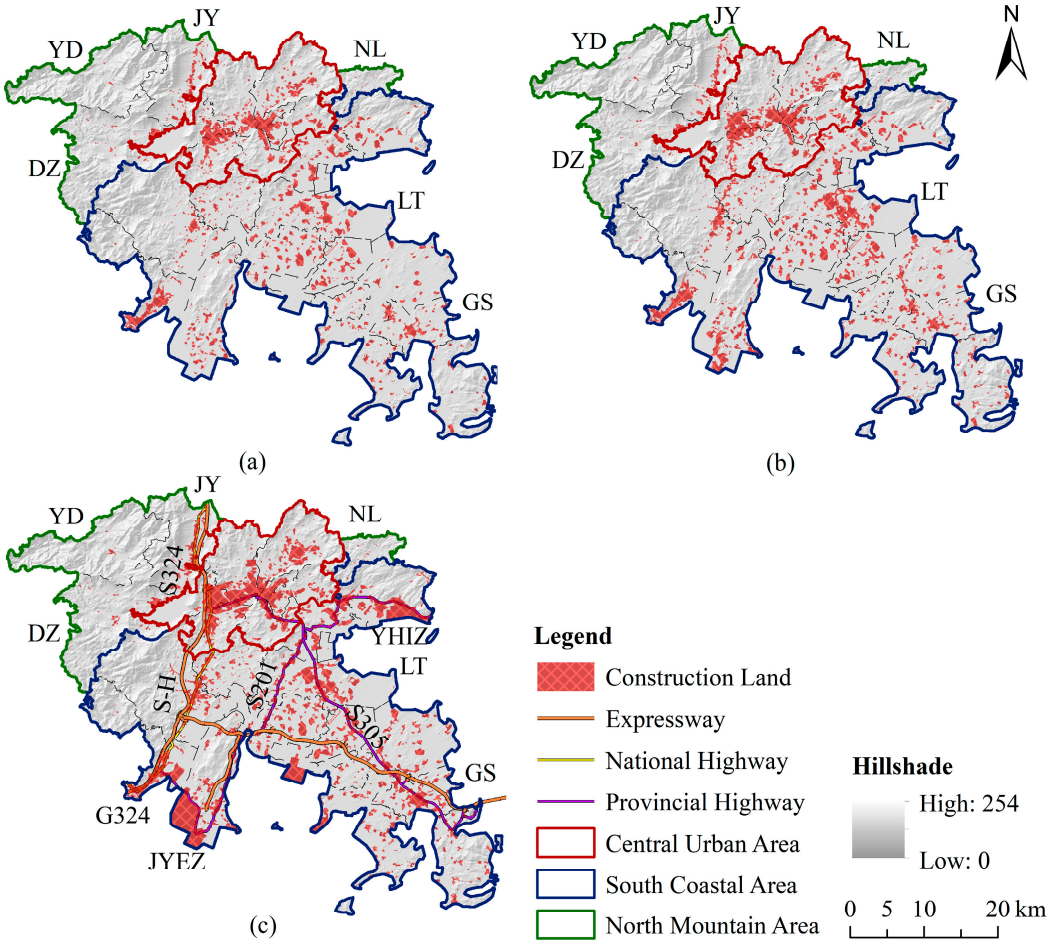


Figure 7. Construction land of study area between 2000 and 2020: (**a**): 2000; (**b**):2010; (**c**): 2020, YHIZ: Yuanhong Investment Zone; JYEZ: Jiangyin Economic Zone; GS: Gaoshan Town, LT: Longtian Town, YD: Yidu Town, DZ: Dongzhang Town, NL: Nanling Town, JY: Jiangyin Town, S-H: Shenyang-Haikou Expressway.

The spillover effect of construction land in the valley near G324 in the northern mountainous area exhibited a "High-High Cluster" initially, but this gradually decreased during the study period. By 2020, there was no significant spatial correlation between construction land and cultivated land. Due to topographical constraints, the expansion of construction land in the western region is limited, resulting in a weak spillover effect on cultivated land, forming a "Low-Low Cluster".

In the past two decades, the spillover effect of construction land in the south coastal area has exhibited a strong "High-High Cluster" pattern, with a limited spillover impact beyond proximate areas resulting in a "Low-High Outlier" trend. However, as of 2010, the spatial correlation was not significant for regions outside those with relatively concentrated construction land. In 2020, the spillover effect of construction land near the Yuanhong

Investment Zone exhibited a weak trend, primarily manifesting as a "High-Low Outlier". Due to the constraints imposed by the northern mountains, the surrounding area displayed a "Low-Low Cluster". Similarly, given that the topography of the southernmost peninsula was predominantly hilly, there was a limited spillover effect observed during this study period.

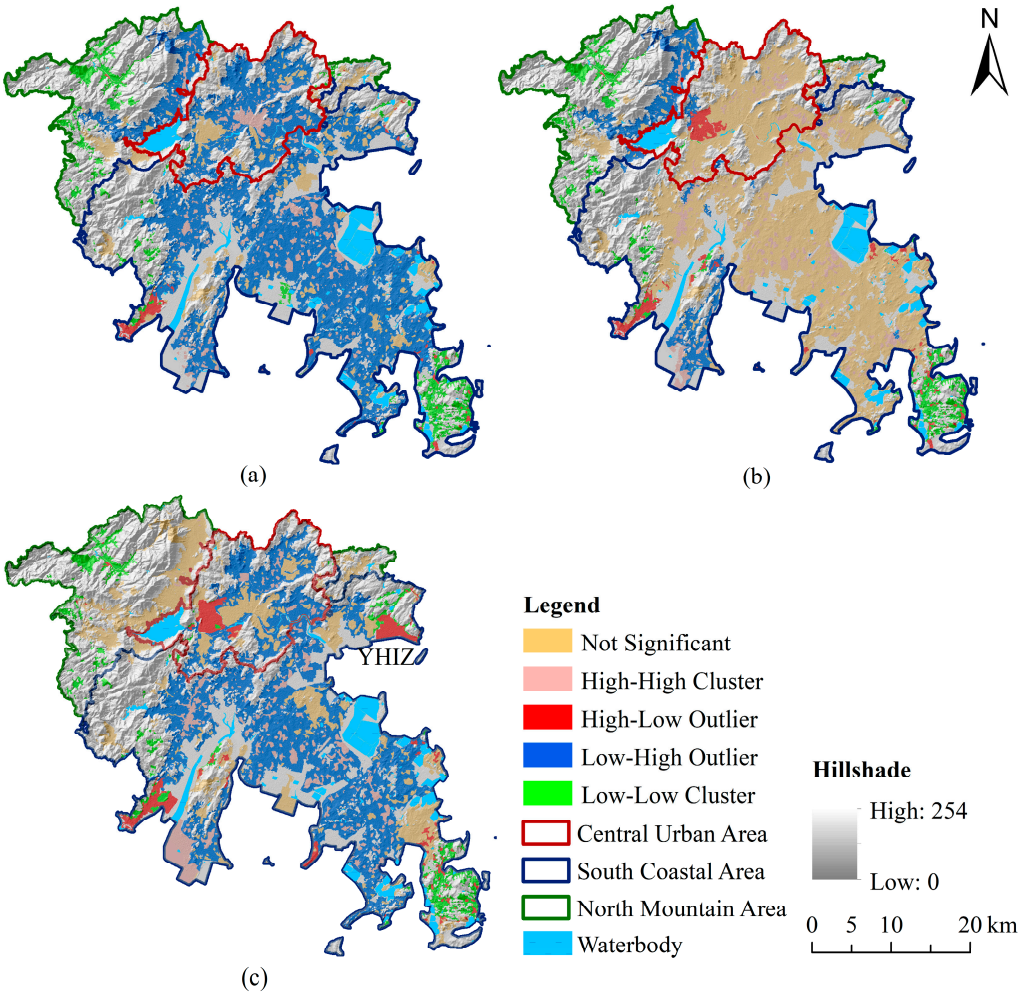


Figure 8. Spatial interaction types of the construction land and cultivated land in the study area: (**a**): 2000; (**b**):2010; (**c**): 2020, YHIZ: Yuanhong Investment Zone.

3.3. Impact of Construction Land Expansion on Cultivated Land Fragmentation

3.3.1. Land Use Transition

The land use transition matrix in the study area showed a remarkable increase in construction land, primarily at the expense of cultivated land (Tables 7 and 8). From 2000 to 2010, a total of 42.79 km^2 of non-construction land was converted into construction land, with cultivated land being the primary source (35.96 km^2, accounting for 84.04%), followed by woodland (5.11 km^2). From 2010 to 2020, a total of 98.51 km^2 of non-construction land was converted into construction land, primarily consisting of cultivated land (68.01 km^2, accounting for 69.04%), followed by waterbodies (14.28 km^2), sea area (8.59 km^2), and others. During the study period, the proportion of cultivated land occupied by construction land for expansion decreased, while the occupied area increased remarkably. During the second decade, a notable number of waterbodies and sea areas were transformed into construction land.

Table 7. Land use transition matrix between 2000 and 2010 (km^2).

Year	Land Use Type	2010 Grassland	Sea Area	Construction Land	Woodland	Bare Ground	Cultivated Land	Wetland	Waterbodies	Total
2000	Grassland	34.92	0.98	0.39	20.01	0.84	4.00	0.12	0.10	61.36
	Sea area	0.06	28.03	0.10	0.19	0.11	0.54	0.71	0.35	30.09
	Construction land	0.25	0.06	109.19	0.57	0.01	14.79	0.09	0.36	125.32
	Woodland	19.16	8.40	5.11	510.08	2.03	17.13	0.27	1.73	563.91
	Bare ground	0.85	0.22	0.23	1.89	3.37	0.60	0.05	0.15	7.36
	Cultivated land	4.60	1.31	35.96	17.29	0.46	607.56	1.20	5.62	674.00
	Wetland	0.08	0.61	0.51	0.23	0.03	1.48	40.49	2.32	45.75
	Waterbodies	0.11	0.44	0.49	1.61	0.14	5.63	2.20	123.15	133.77
	Total	60.03	40.05	151.98	551.87	6.99	651.73	45.13	133.78	1641.56

Table 8. Land use transition matrix between 2010 and 2020 (km^2).

Year	Land Use Type	2020 Grassland	Sea Area	Construction Land	Woodland	Bare Ground	Cultivated Land	Wetland	Waterbodies	Total
2010	Grassland	25.53	0.13	1.04	25.58	0.82	6.57	0.11	0.25	60.03
	Sea area	0.05	3.96	8.59	8.68	0.13	0.68	16.85	1.11	40.05
	Construction land	0.38	0.04	126.25	1.30	0.06	22.62	0.28	1.05	151.98
	Woodland	26.28	0.32	3.27	485.79	1.83	27.27	0.47	6.64	551.87
	Bare ground	0.89	0.26	0.18	3.48	1.06	0.69	0.15	0.28	6.99
	Cultivated land	6.19	0.88	68.01	26.57	0.57	523.40	3.48	22.63	651.73
	Wetland	0.20	0.25	3.14	0.69	0.06	1.77	31.63	7.39	45.13
	Waterbodies	0.17	0.20	14.28	1.56	0.16	6.32	10.70	100.39	133.78
	Total	59.69	6.04	224.76	553.65	4.69	589.32	63.67	139.74	1641.56

Cultivated land has decreased notably and the encroachment of construction land on cultivated land appeared to be the main cause of cultivated land loss. From 2000 to 2010, a total of 66.44 km^2 of cultivated land was converted to other land use types, among which, the main land type converted out was construction land (35.96 km^2, accounting for 54.12%), followed by woodland (17.29 km^2). From 2010 to 2020, a total of 128.33 km^2 of cultivated land was converted to other land use types, among which, construction land was the primary recipient (68.01 km^2, accounting for 53.00%), followed by woodland (26.57 km^2) and waterbodies (22.63 km^2). Hence, it is evident that the area occupied by construction land is more than half of the area converted from cultivated land. Due to the implementation of ecological protection policies, such as the Grain for Green project, woodland has become a major land use type converted from cultivated land. Additionally, woodland has been the primary source of cultivated land supply due to policies aimed at protecting and balancing cultivated land requisition and compensation. Over the course of 20 years, a total of 44.40 km^2 of woodland was converted into cultivated land, followed by construction land (37.41 km^2). However, the area of cultivated land converted into construction land and woodland exceeded the conversion from either woodland or construction land to cultivated use, resulting in an evident decrease in overall cultivated land.

Figure 9 showed that the cultivated land converted to construction land in the first ten years was scattered, with the concentrated conversion taking two forms: linear expansion around G324 and aggregation-type expansion such as Longtian town. In the second decade, the transformation from cultivated land to construction land was predominantly characterized by aggregation, particularly evident in the central urban area and Yuanhong investment zone (YH in Figure 9b). In addition, two distinct linear changes were observed near S201, S305, and G324.

3.3.2. Landscape Pattern

The landscape pattern indices (Table 9) were calculated using the number of patches (NP), patch density (PD), patch area_mean (AREA_MN), aggregation index (AI), and landscape shape index (LSI) for both cultivated land and construction land. Generally, the

changing trends in landscape pattern indices for these two types of land are opposite to each other, as shown by the following analysis.

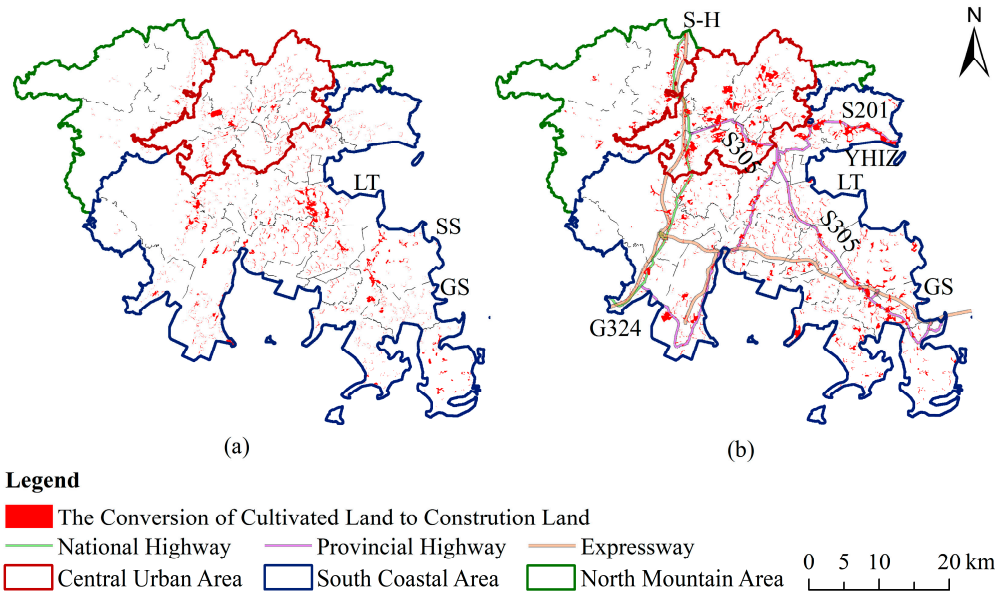


Figure 9. Spatial distribution of the conversion of cultivated land to construction land from 2000 to 2020: (**a**): 2000–2010; (**b**): 2010–2020.

Table 9. Landscape pattern index calculation results of cultivated land and construction land.

Index	Region	Cultivated Land			Construction Land		
		2000 a	2010 a	2020 a	2000 a	2010 a	2020 a
NP (pcs)	Entire study area	306	383	414	694	630	572
	Central urban area	95	104	133	143	130	114
	North mountain area	92	79	96	79	78	70
	South coastal area	201	271	291	483	433	406
PD (pcs/100 ha)	Entire study area	0.19	0.23	0.25	0.42	0.38	0.35
	Central urban area	0.35	0.39	0.49	0.53	0.48	0.42
	North mountain area	0.27	0.23	0.28	0.23	0.23	0.20
	South coastal area	0.20	0.26	0.28	0.47	0.42	0.39
AREA_MN (ha)	Entire study area	220.50	170.40	142.46	18.07	23.99	39.38
	Central urban area	122.99	109.49	72.42	24.99	30.24	49.04
	North mountain area	103.18	119.78	94.89	7.96	8.42	14.16
	South coastal area	229.83	163.63	137.97	17.34	24.46	39.17
AI (%)	Entire study area	95.19	94.92	94.37	90.98	91.70	93.93
	Central urban area	94.80	94.61	93.87	93.00	93.49	95.53
	North mountain area	93.68	93.64	93.25	87.05	87.20	90.21
	South coastal area	95.52	95.14	94.68	90.67	91.46	93.73
LSI (No units)	Entire study area	42.57	44.16	46.51	34.56	34.86	31.29
	Central urban area	19.67	20.09	20.96	14.86	14.53	12.08
	North mountain area	21.46	21.54	22.37	11.64	11.80	11.17
	South coastal area	33.08	35.05	36.45	29.32	30.16	27.27

Note: "a" represents the year.

The NP and PD of the cultivated land in the study area exhibited an upward trend, while AREA_MN demonstrated a downward trend. The changing pattern observed in the central urban and south coastal areas was consistent with that of the overall study area, indicating a gradual fragmentation of large patches of cultivated land and an increase in smaller-patch numbers. Both PD and NP exhibited a decreasing trend followed by an increasing trend, with a greater magnitude of increase than decrease. Conversely,

AREA_MN displayed an opposite pattern, indicating that the fragmentation of cultivated land had improved in this area in 2010. However, it worsened between 2010 and 2020. The LSI of both the study area as a whole and its sub-regions exhibited an upward trend over the past two decades, while the AI displayed a downward trend. Furthermore, the intensity of change during the second decade was almost greater than that observed in the previous decade (with a slightly higher changing intensity of LSI noted in the south coastal area during the first decade). The findings indicated that the cultivated land landscape in the study area exhibits a growing complexity, with an increasing degree of fragmentation and decreasing degree of aggregation.

The PD and the NP of construction land in the entire study area and three subareas exhibited a declining trend, while both the AREA_MN and AI demonstrated an upward trajectory (Table 9). This indicated that with the expansion of construction land, scattered parcels were gradually being connected, resulting in a reduction in their number and an increase in their aggregation. From 2000 to 2010, the north mountain area faced limitations in terms of topography and economy that hindered the expansion of the construction land. Consequently, there was only a slight change in landscape pattern indices (PD being 0.2308% in 2000 and 0.2286% in 2010). However, over the past decade (2010–2020), there has been a much greater range of changes observed for PD, NP, and Area_MN within this area. The motivation for this was that the economic development of the region was accelerated in the latter ten years, which reduced the restrictions of terrain-to-land development, rapidly expanded the construction land, and intensified the fragmentation of the cultivated land landscape.

The LSI of construction land in the entire study area exhibited an initial increase followed by a subsequent decrease during the study period. In the second decade, there was a significant decline, indicating that the construction land expanded rapidly and assumed a more regular shape. The LSI of the central urban area has exhibited a declining trend over the past two decades, with a decrease in the patch separation degree of the construction land primarily due to concentrated expansion. The LSI of the other two areas exhibited an initial increase followed by a subsequent decrease, indicating that the degree of patch separation for the construction land was high during the first decade, but became more dispersed and expanded over time. Additionally, there was a trend towards regularity in the shape of the construction land during the second decade, resulting in a reduction in patch separation.

In addition, Table 9 also showed that the fragmentation of cultivated land in the north mountain area is consistently more severe than that in other areas. Moreover, there are significant regional differences in terms of cultivated land fragmentation, with the order being: northern mountainous area > central urban area > south coastal area. In conclusion, the expansion of construction land resulted in the fragmentation of cultivated land. Topography exerts a greater influence on cultivated land landscape fragmentation than economic factors. However, as the economy develops, topographical constraints on construction land expansion will weaken, intensifying cultivated land landscape fragmentation in mountainous areas.

4. Discussion

This study explored the spatial and temporal characteristics of construction land and cultivated land fragmentation, and analyzed the mechanisms by which construction land expansion affects cultivated land. The findings indicated that the acceleration of construction land expansion has resulted in an increasing loss of cultivated land, the cores of large-scale cultivated land being primarily dispersed in regions characterized by low and flat topography. The expansion of construction land patches has significantly enhanced

connectivity and intensified the trend of cultivated land fragmentation. The degree of fragmentation was found to be highest in the north mountain area, followed by the central urban area and then the south coastal area.

Previous studies have demonstrated that the landscape pattern index is significantly influenced by both terrain and economic factors, with cultivated land fragmentation being more prevalent in hilly regions due to topographical constraints [32,33]. This study area encompasses two types of terrain: plain and mountain. Without differentiation, the accuracy of the calculated landscape pattern indices may be compromised by the influence of varying terrains. Therefore, the study area was divided into three parts, namely, the north mountain area, central urban area, and south coastal area, based on topographic and economic development factors. This division ensured that the landscape pattern indices can accurately reflect regional landscape characteristics, which was beneficial for analyzing the primary causes of cultivated land fragmentation in the study area.

Studies on the fragmentation of cultivated land have primarily focused on overall quantitative analysis using the landscape pattern index. However, to accurately monitor the spatial differences in the landscape fragmentation of cultivated land, it is necessary to analyze the landscape's spatial details. MSPA can provide a comprehensive understanding of the spatial morphological characteristics of the cultivated land landscape. Therefore, this study combined MSPA with zonal calculations of landscape pattern indices. Studies have identified core areas through MSPA when extracting ecological sources and constructing ecological networks [34,35], but they have seldom distinguished core areas in the context of landscape fragmentation. In this study, significant variations were observed in terms of both the number and size of cultivated land core areas across different regions. Therefore, this study categorized the core areas of cultivated land based on their size to facilitate the analysis of factors contributing to fragmentation. Additionally, in the MSPA method, variations in setting the parameters significantly impact the feature morphology and area [36,37]. A uniform edge width of one was set in this study to maximize the core area.

The policy implications of this study encompass the following five key areas: First, it is imperative to control the excessive expansion of construction land through scientifically sound and reasonable land planning. By delineating urban development boundaries, permanent basic farmland, and ecological protection red lines, the uncontrolled expansion of construction land can be strictly restricted, thereby safeguarding cultivated land resources. Second, the government should further enhance its cultivated land protection policies and ensure both the quality and quantity of new cultivated land through the "balance of occupation and compensation" policy. Additionally, cultivated land protection should be integrated into the performance evaluation criteria for local governments, prohibiting the fragmentation caused by the arbitrary occupation of cultivated land. Third, optimizing the layout of urban and rural construction land and shifting the focus of urban development from "expansion" to "intensive use" can effectively control the rate of construction land expansion. Priority should also be given to reclaiming residential land surrounded by cultivated land or in inconvenient locations to achieve large-scale management. Fourth, improving land use efficiency, optimizing the layout of construction land, and minimizing the occupation of cultivated land are essential. Finally, strengthening policy coordination and providing technical support will better enable the assessment and management of the impact of construction land expansion on cultivated land.

Even though this study integrated multiple methods to analyze the impact mechanisms of construction land expansion on cultivated land, it is important to acknowledge its limitations. This study focused on morphological changes in the study of cultivated land fragmentation. The fragmentation of cultivated land involves multiple aspects such as resource allocation, spatial distribution, utilization efficiency, and ownership [38,39]. In the

future, analysis can be conducted from multiple aspects such as the function and quality of cultivated land. In addition, national policies and land spatial planning have a significant impact on future land use conditions [40,41]. Future research can establish predictive models for the expansion of construction land and the fragmentation of cultivated land, providing more scientific and recommendations for policy formulation and planning.

5. Conclusions

This study constructed a framework to explore the impact of construction land expansion on cultivated land fragmentation from the multiple perspectives of morphology, statistics, spatio-temporal characteristics, and landscape patterns. The results found that the core area of cultivated land constituted the predominant landscape element; however, there has been an intensifying trend towards fragmentation, with larger cores dividing into smaller ones. Construction land had a significant spillover effect and was spatially associated with cultivated land. The expansion of construction land encroached on surrounding cultivated areas, leading to the reduced area and irregular shapes of the latter, thereby intensifying landscape fragmentation. Future research can be conducted based on the information obtained in this study to develop models to predict future patterns of cultivated and construction land to provide suggestions for land resource policy making and planning.

Author Contributions: Conceptualization, X.Z. and X.Y. (Xinyang Yu); software, X.Y. (Xiaoran Yang); validation, X.Y. (Xiaoran Yang); field investigation, X.Y. (Xiaoran Yang) and X.Z.; writing—original draft, X.Z.; writing—review and editing, X.Z. and X.Y. (Xinyang Yu). All authors have read and agreed to the published version of the manuscript.

Funding: This study was supported by the National Key Research and Development Program of China (2022YFC3204404). And The APC was funded by the National Key Research and Development Program of China (2022YFC3204404). The supporters have no role in the study design, data collection, decision to publish, or preparation of the article.

Institutional Review Board Statement: Not applicable.

Data Availability Statement: Data used in this study are available upon request.

Acknowledgments: We would like to thank the anonymous reviewers for their constructive comments on the manuscript.

Conflicts of Interest: The authors declare no conflicts of interest.

References

1. Deng, X.; Xu, X.; Cai, H.; Li, J. Assessment the impact of urban expansion on cropland net primary productivity in Northeast China. *Ecol. Indic.* **2024**, *159*, 111698. [CrossRef]
2. Zhang, X.; Song, W.; Lang, Y.; Feng, X.; Yuan, Q.; Wang, J. Land use changes in the coastal zone of China's Hebei Province and the corresponding impacts on habitat quality. *Land Use Policy* **2020**, *99*, 104957. [CrossRef]
3. Wang, W.; Deng, X.; Wang, Y.; Peng, L.; Yu, Z. Impacts of infrastructure construction on ecosystem services in new-type urbanization area of North China Plain. *Resour. Conserv. Recycl.* **2022**, *185*, 106376. [CrossRef]
4. Wu, Y.; Shan, L.; Guo, Z.; Peng, Y. Cultivated land protection policies in China facing 2030: Dynamic balance system versus basic farmland zoning. *Habitat Int.* **2017**, *69*, 126–138. [CrossRef]
5. Guo, J.; Qin, Y.; Du, X.; Han, Z. Dynamic measurements and mechanisms of coastal port–city relationships based on the DCI model: Empirical evidence from China. *Cities* **2020**, *96*, 102440. [CrossRef]
6. Guo, J.; Qin, Y. Coupling characteristics of coastal ports and urban network systems based on flow space theory: Empirical evidence from China. *Habitat Int.* **2022**, *126*, 102624. [CrossRef]
7. Zhang, H.; Chen, M.; Liang, C. Urbanization of county in China: Spatial patterns and influencing factors. *J. Geogr. Sci.* **2022**, *32*, 1241–1260. [CrossRef]

8. Chen, Y.; Li, M.; Zhang, Z. Does the Rural Land Transfer Promote the Non-Grain Production of Cultivated Land in China? *Land* **2023**, *12*, 688. [CrossRef]
9. Zhou, Y.; Li, X.; Liu, Y. Cultivated land protection and rational use in China. *Land Use Policy* **2021**, *106*, 105454. [CrossRef]
10. Zhai, H.; Lv, C.; Liu, W.; Yang, C.; Fan, D.; Wang, Z.; Guan, Q. Understanding spatio-temporal patterns of land use/land cover change under urbanization in Wuhan, China, 2000–2019. *Remote Sens.* **2021**, *13*, 3331. [CrossRef]
11. Zhao, X.; Huang, G. Exploring the impact of landscape changes on runoff under climate change and urban development: Implications for landscape ecological engineering in the Yangmei River Basin. *Ecol. Eng.* **2022**, *184*, 106794. [CrossRef]
12. Zhang, M.; Chen, Q.; Zhang, K. Influence of the variation in rural population on farmland preservation in the rapid urbanization area of China. *J. Geogr. Sci.* **2021**, *31*, 1365–1380. [CrossRef]
13. Qian, F.; Chi, Y.; Lal, R.; Lorenz, K. Spatio-temporal characteristics of cultivated land fragmentation in different landform areas with a case study in Northeast China. *Ecosyst. Health Sustain.* **2020**, *6*, 1800415. [CrossRef]
14. Fu, F.; Deng, S.; Wu, D.; Liu, W.; Bai, Z. Research on the spatiotemporal evolution of land use landscape pattern in a county area based on CA-Markov model. *Sustain. Cities Soc.* **2022**, *80*, 103760. [CrossRef]
15. Su, S.; Jiang, Z.; Zhang, Q.; Zhang, Y. Transformation of agricultural landscapes under rapid urbanization: A threat to sustainability in Hang-Jia-Hu region, China. *Appl. Geogr.* **2011**, *31*, 439–449. [CrossRef]
16. Luo, Y.; Wang, Z.; Zhou, X.; Hu, C.; Li, J. Spatial-Temporal Driving Factors of Urban Landscape Changes in the Karst Mountainous Regions of Southwest China: A Case Study in Central Urban Area of Guiyang City. *Sustainability* **2022**, *14*, 8274. [CrossRef]
17. Velázquez, J.; Gutiérrez, J.; Hernando, A.; García-Abril, A. Evaluating landscape connectivity in fragmented habitats: Cantabrian capercaillie (*Tetrao urogallus cantabricus*) in northern Spain. *For. Ecol. Manag.* **2017**, *389*, 59–67. [CrossRef]
18. Lin, J.; Huang, C.; Wen, Y.; Liu, X. An assessment framework for improving protected areas based on morphological spatial pattern analysis and graph-based indicators. *Ecol. Indic.* **2021**, *130*, 108138. [CrossRef]
19. Riitters, K.H.; Vogt, P.; Soille, P.; Kozak, J.; Estreguil, C. Neutral model analysis of landscape patterns from mathematical morphology. *Landsc. Ecol.* **2007**, *22*, 1033–1043. [CrossRef]
20. Carlier, J.; Moran, J. Landscape typology and ecological connectivity assessment to inform Greenway design. *Sci. Total Environ.* **2019**, *651*, 3241–3252. [CrossRef]
21. Ferrari, B.; Quatrini, V.; Barbati, A.; Corona, P.; Masini, E.; Russo, D. Conservation and enhancement of the green infrastructure as a nature-based solution for Rome's sustainable development. *Urban Ecosyst.* **2019**, *22*, 865–878. [CrossRef]
22. Shi, F.; Liu, S.; An, Y.; Sun, Y.; Dong, S.; Wu, X. Dynamic change of landscape fragmentation and connectivity in the context of urbanization: A case study of Kunming City. *Acta Ecol. Sin.* **2020**, *40*, 3303–3314.
23. Jiang, P.; Chen, D.; Li, M. Farmland landscape fragmentation evolution and its driving mechanism from rural to urban: A case study of Changzhou City. *J. Rural. Stud.* **2021**, *82*, 1–18.
24. Bi, S.; Dai, F.; Chen, M.; Xu, S. A new framework for analysis of the morphological spatial patterns of urban green space to reduce PM2. 5 pollution: A case study in Wuhan, China. *Sustain. Cities Soc.* **2022**, *82*, 103900. [CrossRef]
25. Saura, S.; Vogt, P.; Velázquez, J.; Hernando, A.; Tejera, R. Key structural forest connectors can be identified by combining landscape spatial pattern and network analyses. *For. Ecol. Manag.* **2011**, *262*, 150–160. [CrossRef]
26. Soille, P.; Vogt, P. Morphological segmentation of binary patterns. *Pattern Recognit. Lett.* **2008**, *30*, 456–459. [CrossRef]
27. Wang, Q.; Liu, S.; Liu, Y.; Wang, F.; Liu, H.; Yu, L. Effects of urban agglomeration and expansion on landscape connectivity in the river valley region, Qinghai-Tibet Plateau. *Glob. Ecol. Conserv.* **2022**, *34*, e02004. [CrossRef]
28. Jia, Y.; Tang, L.; Xu, M.; Yang, X. Landscape pattern indices for evaluating urban spatial morphology—A case study of Chinese cities. *Ecol. Indic.* **2019**, *99*, 27–37. [CrossRef]
29. Ma, L.; Bo, J.; Li, X.; Fang, F.; Cheng, W. Identifying key landscape pattern indices influencing the ecological security of inland river basin: The middle and lower reaches of Shule River Basin as an example. *Sci. Total Environ.* **2019**, *674*, 424–438. [CrossRef]
30. Mantyka-pringle, C.S.; Martin, T.G.; Rhodes, J.R. Interactions between climate and habitat loss effects on biodiversity: A systematic review and meta-analysis. *Glob. Change Biol.* **2012**, *18*, 1239–1252. [CrossRef]
31. Lyu, Y.; Wang, M.; Zou, Y.; Wu, C. Mapping trade-offs among urban fringe land use functions to accurately support spatial planning. *Sci. Total Environ.* **2022**, *802*, 149915. [CrossRef] [PubMed]
32. Bai, L.; Xiu, C.; Feng, X.; Liu, D. Influence of urbanization on regional habitat quality: A case study of Changchun City. *Habitat Int.* **2019**, *93*, 102042. [CrossRef]
33. Shi, Z.; Ma, L.; Zhang, W.; Gong, M. Differentiation and correlation of spatial pattern and multifunction in rural settlements considering topographic gradients: Evidence from Loess Hilly Region, China. *J. Environ. Manag.* **2022**, *315*, 115127. [CrossRef] [PubMed]
34. Li, Y.-Y.; Zhang, Y.-Z.; Jiang, Z.-Y.; Guo, C.-X.; Zhao, M.-Y.; Yang, Z.-G.; Guo, M.-Y.; Wu, B.-Y.; Chen, Q.-L. Integrating morphological spatial pattern analysis and the minimal cumulative resistance model to optimize urban ecological networks: A case study in Shenzhen City, China. *Ecol. Process.* **2021**, *10*, 63. [CrossRef]

35. Huang, K.; Peng, L.; Wang, X.; Deng, W. Integrating circuit theory and landscape pattern index to identify and optimize ecological networks: A case study of the Sichuan Basin, China. *Environ. Sci. Pollut. Res.* **2022**, *29*, 66874–66887. [CrossRef]
36. Ostapowicz, K.; Vogt, P.; Riitters, K.H.; Kozak, J.; Estreguil, C. Impact of scale on morphological spatial pattern of forest. *Landsc. Ecol.* **2008**, *23*, 1107–1117. [CrossRef]
37. Xu, L.; Yu, H.; Zhong, L. Evolution of the landscape pattern in the Xin'an River Basin and its response to tourism activities. *Sci. Total Environ.* **2023**, *880*, 163472. [CrossRef]
38. Xu, W.; Jin, X.; Liu, J.; Zhou, Y. Analysis of influencing factors of cultivated land fragmentation based on hierarchical linear model: A case study of Jiangsu Province, China. *Land Use Policy* **2021**, *101*, 105119. [CrossRef]
39. Fei, R.; Lin, Z.; Chunga, J. How land transfer affects agricultural land use efficiency: Evidence from China's agricultural sector. *Land Use Policy* **2021**, *103*, 105300. [CrossRef]
40. Hurlimann, A.; Moosavi, S.; Browne, G.R. Urban planning policy must do more to integrate climate change adaptation and mitigation actions. *Land Use Policy* **2021**, *101*, 105188. [CrossRef]
41. Brown, G.; Sanders, S.; Reed, P. Using public participatory mapping to inform general land use planning and zoning. *Landsc. Urban Plan.* **2018**, *177*, 64–74. [CrossRef]

Disclaimer/Publisher's Note: The statements, opinions and data contained in all publications are solely those of the individual author(s) and contributor(s) and not of MDPI and/or the editor(s). MDPI and/or the editor(s) disclaim responsibility for any injury to people or property resulting from any ideas, methods, instructions or products referred to in the content.